ERL-0180-TM AR 002 090

DEPARTMENT OF DEFENCE

DEFENCE SCIENCE AND TECHNOLOGY ORGANISATION

ELECTRONICS RESEARCH LABORATORY

DEFENCE RESEARCH CENTRE SALISBURY
SOUTH AUSTRALIA

TECHNICAL MEMORANDUM

ERL-0180-TM

THE MEASUREMENT AND SIMULATION OF THE LIGHT OF THE NIGHT SKY

M.S. BROWN

Approved for Public Release

COPY No. 13

JANUARY 1981

AR-002-090

DEPARTMENT OF DEFENCE

DEFENCE SCIENCE AND TECHNOLOGY ORGANISATION

ELECTRONICS RESEARCH LABORATORY

(9) TECHNICAL MEMORANDUM

(14) ERL-0180-TM

THE MEASUREMENT AND SIMULATION OF THE LIGHT OF THE NIGHT SKY

(10) M.S. Brown M.Sc.

(12) 27

SUMMARY

A description is given of the spectral distribution and origins of the light of the night sky. Details are provided of the design of a filter for use with a tungsten filament light source to produce a spectral distribution similar to that of the moonless night sky. The level of illumination from the filtered light source was set by reference to radiometer measurements of the night sky made at a remote coastal location.

(1) Jan 81

POSTAL ADDRESS: Chief Superintendent, Electronics Research Laboratory, Box 2151, GPO, Adelaide, South Australia, 5001.

DOCUMENT CONTROL DATA SHEET

Security classification of this page: UNCLASSIFIED

1 DOCUMENT NUMBERS	2 SECURITY CLASSIFICATION
AR Number: AR-002-090	a. Complete Document: Unclassified
Report Number: ERL-0180-TM	b. Title in Isolation: Unclassified
Other Numbers:	c. Summary in Isolation: Unclassified

3 TITLE

THE MEASUREMENT AND SIMULATION OF THE LIGHT OF THE NIGHT SKY

4 PERSONAL AUTHOR(S):	5 DOCUMENT DATE:
M.S. Brown	January 1981
	6 6.1 TOTAL NUMBER OF PAGES 20
	6.2 NUMBER OF REFERENCES: 11

7 7.1 CORPORATE AUTHOR(S):	8 REFERENCE NUMBERS
Electronics Research Laboratory	a. Task: ALL 99/006
	b. Sponsoring Agency: NAVY 6/77
7.2 DOCUMENT SERIES AND NUMBER Electronics Research Laboratory 0180-TM	9 COST CODE:

10 IMPRINT (Publishing organisation)	11 COMPUTER PROGRAM(S) (Title(s) and language(s))
Defence Research Centre Salisbury	

12 RELEASE LIMITATIONS (of the document):

Approved for Public Release

12.0 OVERSEAS	NO	P.R. 1	A	B	C	D	E

Security classification of this page: UNCLASSIFIED

Security classification of this page: UNCLASSIFIED

13 ANNOUNCEMENT LIMITATIONS (of the information on these pages)

No limitation

14 DESCRIPTORS:

a. EJC Thesaurus Terms

Night sky
Moonlight
Nightglow
Starlight
Darkness
Light (visible radiation)
Filters
Light sources
Radiometry
Spectral energy distribution
Twilight glow
Sky brightness
Measurement
Simulation

b. Non-Thesaurus Terms

15 COSATI CODES:

0401
2006

16 LIBRARY LOCATION CODES (for libraries listed in the distribution):

17 SUMMARY OR ABSTRACT:
(if this is security classified, the announcement of this report will be similarly classified)

A description is given of the spectral distribution and origins of the light of the night sky. Details are provided of the design of a filter for use with a tungsten filament light source to produce a spectral distribution similar to that of the moonless night sky. The level of illumination from the filtered light source was set by reference to radiometer measurements of the night sky made at a remote coastal location.

Security classification of this page: UNCLASSIFIED

TABLE OF CONTENTS

LIST OF TABLES

LIST OF FIGURES

1. INTRODUCTION

During the hours of darkness the level of horizon luminance measured from the earths surface depends on the time, location, the phase of the moon and the meteorological conditions. The highest luminance measured is approximately 10^{-2} cd/m^2 when there is a full moon and a cloudless sky, and this drops to about 10^{-3} cd/m^2 on clear starlit nights (see for instance reference 1). Lower levels of luminance are encountered on cloudy nights. Table 1 indicates how the light level varies over the full range of day and night time conditions.

TABLE 1. APPROXIMATE VALUES OF THE LUMINANCE OF THE SKY NEAR THE HORIZON

Conditions	Luminance (cd/m^2)
Clear day	10^4
Overcast day	10^3
Heavily overcast day	10^2
Sunset, overcast day	10
1/4 hour after sunset, clear	1
1/2 hour after sunset, clear	10^{-1}
Fairly bright moonlight	10^{-2}
Moonless, clear night sky	10^{-3}
Moonless, overcast night sky	10^{-4}

As the light level changes due to the phases of the moon the spectral distribution also changes because the light from the moon is reflected sunlight while the radiance of the moonless night sky is due to several sources, some of which differ markedly from sunlight. Averaged throughout the year half the night hours are moonless.

When performing laboratory tests on image intensifiers or purely optical night vision equipment it is important to use the correct light level and spectral distribution because the detector performance is usually a function of the light level and wavelength. Lens aberrations and antireflection coating losses are also wavelength dependent.

This memorandum describes the design of a filter for use with a tungsten filament lamp as a light source for MTF testing of image intensifier night aids and also as a light source for use in resolution tests in the dark tunnel facility maintained at ERL. The filter produces a spectral distribution similar to the moonless night sky and the level of illumination has been set using radiometer measurements of the night sky made over water on moonless nights.

2. THE SOURCES OF THE NIGHT SKY SPECTRAL RADIANCE

2.1 General description

Measurements of the spectral radiance of the night sky have been made in several locations(ref.2,3,4) and two representative sets of data are shown in figure 1. The solid lines show the night sky spectral radiance measured at Lake Montauban, Canada in October 1968, for nights with no moon and also for various phases of the moon(ref.2). These measurements included radiation from the complete hemisphere. The dotted curve gives the average result of a series of measurements of the moonless night sky in October/November 1968 at Pitzal in Austria(ref.3). This curve shows the upper and lower levels of the more prominent night sky line spectra measured during the period, as well as the continuum. The radiometer used for these latter measurements had a field of view of 1.14×10^{-4} steradians and it was directed at an elevation angle of 45° in a direction near SSE.

The spectral character of the night sky on moonless nights is quite unlike that of sunlight, being the result of radiation from the following sources:

(1) Integrated stellar radiation from stars and other galactic sources

(2) Zodiacal light

(3) Airglow

(4) Integrated nebular radiation from distant gaseous nebulae

(5) Auroral emissions (at high latitudes)

The components of the night sky radiation have varying effects on the measured radiance and its spectral distribution depending on the observation position, the sidereal time, the transmission of the atmosphere and the field of view of the measuring instrument. A brief description of the variations in the more important sources is given here and a more complete treatment can be found in reference 5.

2.2 Stellar radiation

On moonless nights the 6000 stars brighter than magnitude 6 that are visible to the naked eye are the most striking feature of the night sky, but stellar radiation contributes only 22% of the total incident visible radiation. In general the number density of the stars in the sky is greatest near the milky way (near the zenith and in a broad band from east to west) and there are relatively few stars to the north and south of this area. For stars brighter than magnitude 30 the number density increases with magnitude (larger magnitudes are dimmer). The light emitted by stars is red shifted compared to sunlight as shown in figure 2. The light from the more distant stars (approximately 10^{11} stars in our galaxy) is attenuated by interstellar dust and also red shifted to a greater degree than the light from the nearer, brighter, but less numerous stars.

2.3 Zodiacal light

The zodiacal light is sunlight scattered by interplanetary dust, mainly in orbit around the sun. The dust gravitates towards the planes of the planetary orbits and its density increases towards the sun, giving rise to a concentration of zodiacal light in the ecliptic (the apparent yearly path traced by the sun on the celestial sphere). The radiance is a function of ecliptic latitude and longitude and it has the same spectral distribution as sunlight (figure 2). Table 2 gives the magnitude of the zodiacal light

at 0.55 μm as a function of latitude and longitude compared to the sun's apparent position(ref.5).

At visual wavelengths the zodiacal light contributes about 44% of the total moonless night irradiance.

TABLE 2. ZODIACAL LIGHT AS A FUNCTION OF ECLIPTIC COORDINATES

(β Latitude, $\Lambda - \Lambda_0$ Longitude)
Units are 10^{-10} W.cm^{-2}.sr^{-1}.μm^{-1}

$\Lambda-\Lambda_0$ \ β	0°	10°	20°	30°	40°	50°	60°	70°	80°
180°(Nadir)	2.58	2.12	1.83	1.59	1.41	1.27	1.17	1.10	1.03
160	2.11	1.94	1.74	1.53	1.37	1.27	1.20	1.12	1.05
140	2.07	1.85	1.68	1.52	1.37	1.28	1.20	1.12	1.05
120	2.39	2.17	1.96	1.77	1.61	1.46	1.32	1.20	1.08
100	2.77	2.47	2.20	1.96	1.75	1.56	1.39	1.23	1.11
80	3.65	3.12	2.58	2.19	1.90	1.66	1.46	1.27	1.11
65	5.35	4.18	3.30	2.58	2.04	1.65	1.37	1.18	1.06
60	6.30	4.55	3.39	2.70	2.12	1.66	1.37	1.20	1.07
55	7.56	5.12	3.58	2.82	2.29	1.83	1.47	1.24	1.07
50	9.39	6.03	4.03	2.90	2.27	1.85	1.49	1.24	1.08
45	1.19x10	6.96	4.42	3.04	2.33	1.89	1.50	1.24	1.07
40	1.49x10	8.25	5.12	3.31	2.40	1.86	1.49	1.26	1.11
35	2.01x10	1.15x10	6.35	3.63	2.24	1.71	1.37	1.18	1.07
30	2.94x10	1.55x10	8.00	4.17	2.41	1.80	1.41	1.20	1.06
25	4.66x10	1.82x10	9.32	4.91	2.46	1.83	1.44	1.21	1.08
20	7.69x10	2.14x10	1.07x10	5.42	2.52	1.86	1.45	1.21	1.08
15	$1.51x10^2$	2.76x10	1.12x10	5.92	2.65	1.90	1.45	1.21	1.08
10	$3.65x10^2$	2.72x10	1.39x10	6.55	2.90	1.99	1.45	1.21	1.08
5	$1.76x10^3$	5.63x10	1.70x10	7.24	3.15	2.09	1.46	1.21	1.08
0(Zenith)	$1.63x10^6$	$1.99x10^2$	2.29x10	7.94	4.03	2.52	1.50	1.21	1.08

Note: For $\beta = 90°$, flux is $0.98x10^{-10}$ W.cm^{-2}.sr^{-1}.μm^{-1}

2.4 Airglow

The airglow is almost completely the result of chemi-luminescent reactions occurring in the upper atmosphere at altitudes of 80 to 110 km. It has been the subject of extensive research and there are several recent papers which give comprehensive reviews on the subject (see for instance references 6, 7 and 8). The complexity of the airglow emissions is due to the variability of the concentration and composition of atmospheric constituents (atoms, molecules and ions) as well as the energy of the extra-terrestrial photons and other particles which interact with the atmosphere at various altitudes in the presence of a variable electromagnetic field. The question of exactly how the various airglow emissions are produced and exactly at what height in the atmosphere is still not completely resolved because there are multiple excitation and de-exitation processes which are responsible for atmospheric emissions under different dynamic conditions of the terrestrial atmosphere.

Figure 3 shows a simplified representation of the airglow spectrum(ref.5). Higher resolution measurements(ref.7) show a multitude of line spectra superimposed on the continuum and the most intense night sky lines are shown on the figure.

The irradiance at the earth's surface due to the airglow can be calculated assuming that it originates from a hollow radiating spherical layer. The radiance measured at ground level varies with the zenith angle due to the geometry of the radiating layer and also due to atmospheric absorption. To a first approximation it is given by

$$I_\theta = I_o T_\theta \sec \theta \qquad (1)$$

where T_θ is the atmospheric transmission along the path.

θ is the zenith angle.

I_o is the zenith spectral radiance due to airglow.

In the visible region of the spectrum the airglow contributes about 33% to the average visible night sky radiation. However, when the horizon is being viewed by an instrument with a restricted field of view the contribution due to airglow will be much greater than this as shown by equation (1), eg

$$I_{80^\circ} = 5.76 I_{0^\circ} T_\theta$$

2.5 Sources outside the galaxy

It is estimated that approximately 10^9 galaxies can be observed in the night sky of which 10^7 are brighter than magnitude 18, but they only contribute about 1% to the total night sky radiance. Galactic light is red shifted with a similar spectrum to stellar radiation.

3. DESIGN OF NIGHT SKY FILTER

The light level required for the laboratory MTF and resolution measurements corresponded to starlight conditions (no moon), which has a spectral distribution as shown by figure 4 curve A. The presence of cloud cover lowers the radiance of the night sky, but does not change the spectral distribution at wavelengths away from the strong H_2O atmospheric absorption lines(ref.3).

A tungsten filament lamp was chosen as the light source for the starlight simulator because a suitable microscope lamp with the required type of filament was available for the MTF low light level test system, and the existing dark tunnel projector used a projector lamp with a tungsten filament. The spectral output from a tungsten filament lamp at a temperature of 2700°K is shown as curve B on figure 4.

The filter transmission characteristic T_λ necessary to match the spectral distribution of the lamp to that of the night sky was obtained from the ratio of the two curves (A and B) shown on figure 4. The lamp output rises continuously as the wavelength increases, so the filter required has its

transmission as high as possible at the short wavelength end of the spectral range to give the maximum amount of transmitted radiation.

The filter transmission characteristic required was calculated from

$$T_\lambda = \frac{H_1}{H_\lambda} \times \frac{S_\lambda}{S_1}$$

where H_1 and H_λ are the values of the lamp output; H_1 being the emission at the shortest wavelength considered and S_1 and S_λ are the values of the starlight spectral radiance; S_1 being the value at the shortest wavelength.

The major part of the transmission characteristic was generated by a 1 mm thickness of Schott BG23 (figure 5 curve A) with an additional 1.5 mm thickness of Corning CS164 (figure 5 curve B) to lower the transmission in the 500 nm to 700 nm region. The short wavelength transmission was further trimmed by the use of a semi-transparent thin film interference filter, vacuum deposited with 7 alternate $\lambda/4$ layers of Schott 8329 deposition glass and zirconium dioxide, deposited at a control wavelength of 500 nm to give the transmission curve shown by figure 5 curve C. The measured transmission curve of the complete filter is shown as figure 5 curve D and can be compared with the required filter shape plotted for discrete points at 50 nm intervals. The main departure from the required curve is in the wavelength range from 650 nm to 750 nm and is due to the low transmission of CS164 in this region. The effect of departures from the required spectral emission will be dealt with in Section 6.

The spectral output of the lamp in combination with the filter is shown by figure 4 curve C.

4. HEAT FILTER

The lamp house used in the dark tunnel is a modified slide projector consisting of a tungsten filament projector lamp, a heat absorbing glass filter, a projection lens and a set of three filter wheels each containing six metal film neutral density filters which can be selected to attenuate the output beam to the required level(ref.9). The heat filter previously used in the projector has a transmission curve as shown in figure 6. This is unsuitable for the simulation of starlight conditions because it significantly modifies the spectral properties of the source, particularly at wavelengths above 700 nm so it was replaced with a neutral density filter consisting of a Rhodium film vacuum deposited onto a 2 mm thick silica disc. A 250 W projector lamp had been used with the absorbtion glass heat filter but this was changed to 150 W when the Rhodium filter was fitted. The transmission of the metal film was chosen so that the total energy passed by the filter in combination with the 150 W lamp was approximately the same as the energy passed by the absorption glass filter with the 250 W lamp. This energy, E, is given by the numerical integration

$$E = \int_{\lambda=0.4\ \mu m}^{\lambda=2.7\ \mu m} H_\lambda . T_\lambda . d\lambda$$

Where H_λ is the spectral output from the lamp and T_λ is the heat filter transmission. The limits of integration were chosen to match the approximate transmission range of the projector lens.

This calculation showed that the absorption glass filter transmitted 5.3% of the energy emitted by the 250 W lamp into the projector lens. When the filter was changed and the lamp power was reduced to 150 W a neutral density filter with a near constant transmission of 9.0% over the wavelength range from 0.4 μm to 2.7 μm was chosen so that the total energy passed to the projector lens was approximately the same as that transmitted by the glass heat filter in combination with the 250 W lamp. This reduced the luminance levels available from the projector because the heat filter transmission in the visible region of the spectrum was reduced from approximately 80.0% to 9.0% as shown on figure 6. With the new heat filter fitted the maximum light level that could be simulated with the dark tunnel projector corresponded to the horizon luminance during twilight, which is brighter than the levels normally used during tests of night vision equipment.

5. NIGHT SKY RADIOMETER MEASUREMENTS

5.1 Description of radiometer

A Schematic drawing of the radiometer used for the night sky measurements is shown in figure 7. Light from the night sky is focussed by the 300 mm focal length lens L onto the photocathode of an EMI 9558 photomultiplier tube which is stopped down to 19 mm diameter to give a field of view of 3.6°. The short wavelength response of the detector (figure 8) is cut at 400 nm by a high pass filter F made from 2 mm thick Schott GG420 glass to shield the detector from short wavelength radiation from the night sky. This is done because the radiation from the dark tunnel projector does not contain any significant energy at wavelengths below 400 nm, as the lamp emission is low at that wavelength (H_λ < 3% of emission at peak wavelength) and the glass components of the lenses used in the dark tunnel projector and image intensifier objective lenses have reduced transmission at wavelengths below 400.0 nm. Any small biases introduced by the low output of the projector at short wavelengths compared to natural starlight can be compensated by calculation.

The removable end cap on the lens tube contains a tritium (Beta particle/phosphor) light source which, when fitted, is used as a standard lamp for setting the photomultiplier EHT voltage. The spectral emission curve for the "Beta" lamp is shown in figure 8. The photomultiplier signal level produced by the standard lamp was set initially by the use of neutral density filters so that it was approximately the same level as that produced by natural starlight.

The photomultiplier was used in a DC measuring mode with the voltage developed across a 1 MΩ anode load monitored with a digital multimeter having a 10 MΩ input impedance. The 1000 V EHT supply was run from a 400 Hz, 12 V DC to 240 V AC inverter that provided adequate stability over the short measuring periods involved.

5.2 Field measurements

Night sky radiance measurements were made at Waitpinga beach on the southern ocean coast of South Australia 80 km south of Adelaide. The measuring site was a south facing sandy bay surrounded by low hills that screened the radiometer from artificial lights.

Figure 9 shows the results of a series of measurements made on the night of 10 April 1980 when sunset occurred at 1742 hours and moonrise at 0047 hours on 11 April 1980. The radiometer was used to measure the broad band sky radiance at 10° elevation angle intervals from the horizon to the zenith at a variety of azimuth angles near due south. Near the southern horizon there was a noticeable sky glow that diminished during the measuring period as shown in the results. Also evident in the readings is the effect of the higher density of stars in the milky way which increased the radiometer reading at elevation angles between 60° and 70°.

Readings were also taken on two other nights but for various reasons the results were unsatisfactory. On the night of 22 January 1980 frontal cloud covered the measuring area shortly before the radiometer was to be used. A single reading of the clear sky was made before the sky clouded over completely and this reading is also shown on figure 9. Another set of readings was made on the night of 9 January 1980 but there was insufficient time between sunset (2024) and moonrise (0008 on 10 January 1980) and the radiometer gave higher than normal readings because of the effects of zodiacal light.

5.3 Dark tunnel measurements

Photometric measurements of the levels of target illumination from the dark tunnel projector were made by the optical radiometry section(ref.10) and the results are shown in Table 3. This gives the photometric transmission of the various filter combinations available from the three, six position filter wheels, and the measured illumination 6 m from the front of the projector.

TABLE 3. CALIBRATION OF DARK TUNNEL PROJECTOR

Light level	Filter wheel settings			Attenuating filter transmissions		Illumination at 6 m from front of glass plate of lamphouse (Lumens/m^2)
	A	B	C	T	Log $\frac{I}{T}$	
0	6	6	6	1.00	0	5.84×10^{-1}
1	6	6	5	3.49×10^{-1}	0.46	2.04×10^{-1}
2	6	5	6	9.20×10^{-2}	1.04	5.37×10^{-2}
3	6	6	4	9.13×10^{-2}	1.04	5.33×10^{-2}
4	6	5	5	3.44×10^{-2}	1.46	2.00×10^{-2}
5	5	6	6	1.13×10^{-2}	1.95	6.62×10^{-3}
6	6	4	6	8.00×10^{-3}	2.10	4.67×10^{-3}
7	6	6	3	6.81×10^{-3}	2.17	4.00×10^{-3}
8	5	6	5	4.05×10^{-3}	2.39	2.37×10^{-3}
9	6	3	6	1.14×10^{-3}	2.94	6.66×10^{-4}
10	4	6	6	1.20×10^{-3}	2.92	7.00×10^{-4}
11	6	5	3		3.2 *	
12	4	6	5	4.33×10^{-4}	3.36	2.53×10^{-4}
13	5	5	5		3.45*	
14	4	5	6	1.23×10^{-4}	3.91	7.17×10^{-5}
15	5	6	3		4.1 *	
16	4	5	5	4.51×10^{-5}	4.35	2.63×10^{-5}

* Values interpolated from measured data

NOTE: Position 6 in each filter wheel is a clear aperture.

The filter combination required to produce a similar radiance from the dark tunnel target background to that measured for the horizon sky in conditions of clear starlight was determined by use of the radiometer.

Before the above comparative measurements were made the radiance factor of the white painted wall was measured to ensure that no major colour biases were introduced when the light from the dark tunnel projector was reflected by the end wall. The radiance factor is the reflectivity of the test sample at a given angle of incidence compared to the reflectivity of a standard Lambertian reflector. Figure 10 shows the radiance factor of the white paint and also that of a grey paint used to produce low contrast Landolt C targets. The radiance factor is approximately constant over the wavelength range of the detectors apart from the 15% dip near 700 nm, which is a characteristic of the paint pigment.

For the comparative measurements the radiometer was set up in the dark tunnel 5 m from the normal target position so that the radiometer field of view was completely filled by the illuminated end wall of the tunnel. It was tripod mounted on one side of the tunnel so that no shadows were cast by the projector beam.

Measurements of the broad band radiance of the tunnel end wall were made while it was irradiated with light from the projector. The results of these measurements are listed in Table 4 and the radiometer readings for the light levels near "clear starlight" (levels 7 to 10) are also shown on figure 9. The conclusion drawn from the measurements was that filter combination No.8 produced a radiance from the dark tunnel end wall similar to that produced by the natural horizon on clear moonless nights.

TABLE 4. RADIOMETER READINGS IN DARK TUNNEL

Projector filter setting		Radiometer reading (mV)		
Level	Filter combination	24/1/80	5/2/80	10/4/80
5	566	187.0		186.0
6	646	144.0		139.0
7	663	140.0		137.0
8	565	67.0	65.0	68.0
9	636	-	48.0	51.0
10	466	21.0	18.9	20.5
11	653	-	14.7	14.5
12	465	7.6	7.5	7.5
13	555	-	7.0	7.0
14	456	2.8	2.5	2.0
15	563	-	2.2	1.65
16	455	1.4	1.4	1.8

6. DETECTOR RESPONSE TO THE LABORATORY LIGHT SOURCE

A comparison between the spectral output from the laboratory light source and the measured spectral radiance of the moonless night sky (figure 4) shows some small differences, notably below 450 nm, between 650 nm and 750 nm and also above 925 nm. These departures from the required curve are small compared to the normal variations that occur in the radiance of the night sky due to airglow and zodiacal light, but an estimate of their importance has been made by numerical integration. The light source was used with a variety of detectors including the dark adapted eye (scotopic response) and photocathode types S20 and S25. The response of each of these detectors to the natural night sky illumination, to the filtered dark tunnel light source and to the unfiltered lamp were calculated and expressed as a ratio showing their response to the lamp sources compared to their response to the night sky.

Thus

$$\frac{R_L}{R_N} = \frac{\int_{\lambda_1}^{\lambda_2} D_\lambda . SL_\lambda . d\lambda}{\int_{\lambda_1}^{\lambda_2} D_\lambda . S_\lambda . d\lambda}$$

where SL_λ is the output of the laboratory light source, S_λ is the spectral radiance of the moonless night sky, and D_λ is the detector spectral sensitivity. The limits of integration were chosen to match the sensitive wavelength range of each detector. The results of the calculations are shown in Table 5 below. The radiometer was used as the standard detector and a scaling factor was calculated to normalise this result by adjusting the values of S_λ used in the integration. This was then used in the calculation of the other detector responses.

TABLE 5. DETECTOR RESPONSE TO FILTERED AND UNFILTERED LAMPS

Detector type	RF/RN	RL/RN
Scotopic eye response	1.08	0.83
S20 photocathode	0.96	1.22
S25 photocathode	0.93	1.59
Radiometer (modified S20)	1.00	1.00

where RF is detector response to the filtered light source

RL is detector response to the unfiltered lamp

RN is detector response to the natural night sky

The table shows that the dark tunnel light source slightly favours the dark adapted eye response compared to the photocathodes, while the unfiltered lamp clearly favours the photocathodes over the dark adapted eye. This factor is nearly 200% for the S25 photocathode.

The dark tunnel light source has been used during low light level resolution tests on a variety of purely optical telescopes and image intensifier night aids and the results have shown good agreement with results obtained using natural night sky illumination(ref.11).

7. CONCLUSIONS

A filter has been made for use with a tungsten filament lamp to produce a spectral distribution similar to the moonless night sky. When used in the dark tunnel projector, the level of illumination from the light source was set by comparison with radiometer measurements of the night sky in a remote beach location.

The response of various detectors to the filtered light source and to the natural night sky has been calculated showing that the detector response to each is similar. The light source has given results in good agreement with field trial results when used during resolution tests in the dark tunnel.

NOTATION

D_λ	normalised detector spectral sensitivity
E	energy
H_λ	spectral output from tungsten filament lamp
I	spectral radiance due to airglow
RF	response of detector to filtered light source
RL	response of detector to unfiltered lamp
RN	response of detector to moonless night sky
SL_λ	normalised output from laboratory light source
S_λ	spectral radiance of starlight
T	transmission
T_λ	transmission of heat filter
Λ	ecliptic longitude
β	ecliptic latitude
θ	zenith angle
λ	wavelength

REFERENCES

No.	Author	Title
1	Knowles-middleton, W.E.	"Vision through the atmosphere". University of Toronto Press, 1952, p.91
2	Vatsia, M.L.	"Atmospheric optical environment". Research and Development Technical Report ECOM-7023, SWM 297224, September 1972
3	Höhn, D.H. and Büchtemann, W.	"Spectral radiance in the S20-range and luminance of the clear and overcast night sky". Applied Optics Vol.12, No.1, June 1973
4	Knestrick, G.L. and Curcio, J.P.	"Measurement of spectral radiance of the horizon sky". NRL Report 6615, December 1967
5	Daniels, G.M.	"A night sky model for satellite search systems". Optical Engineering Vol.16, No.1, January/February 1977
6	Roach, F.E.	"The light of the night sky astronomical interplanetary and geophysical". Space Science Reviews Vol.3, p.512-540, 1964
7	Broadfoot, A.L.	"The airglow spectrum 3100-10,000 Å ". Journal of Geophysics Research Vol.73, No.1, January 1968
8	Chamberlain, J.W.	"Physics of the aurora and airglow". Academic Press 1961
9	Meharry, M.R.	"A dark tunnel optical and thermal test facility". WRE Annual Report 1971/72
10	Brophy, H.J.	Unpublished report on radiometric measurements of dark tunnel projector
11	Brown, M.S.	"The laboratory assessment of image intensifier night aids for use on submarine periscopes". ERL-0176-TR, November 1980

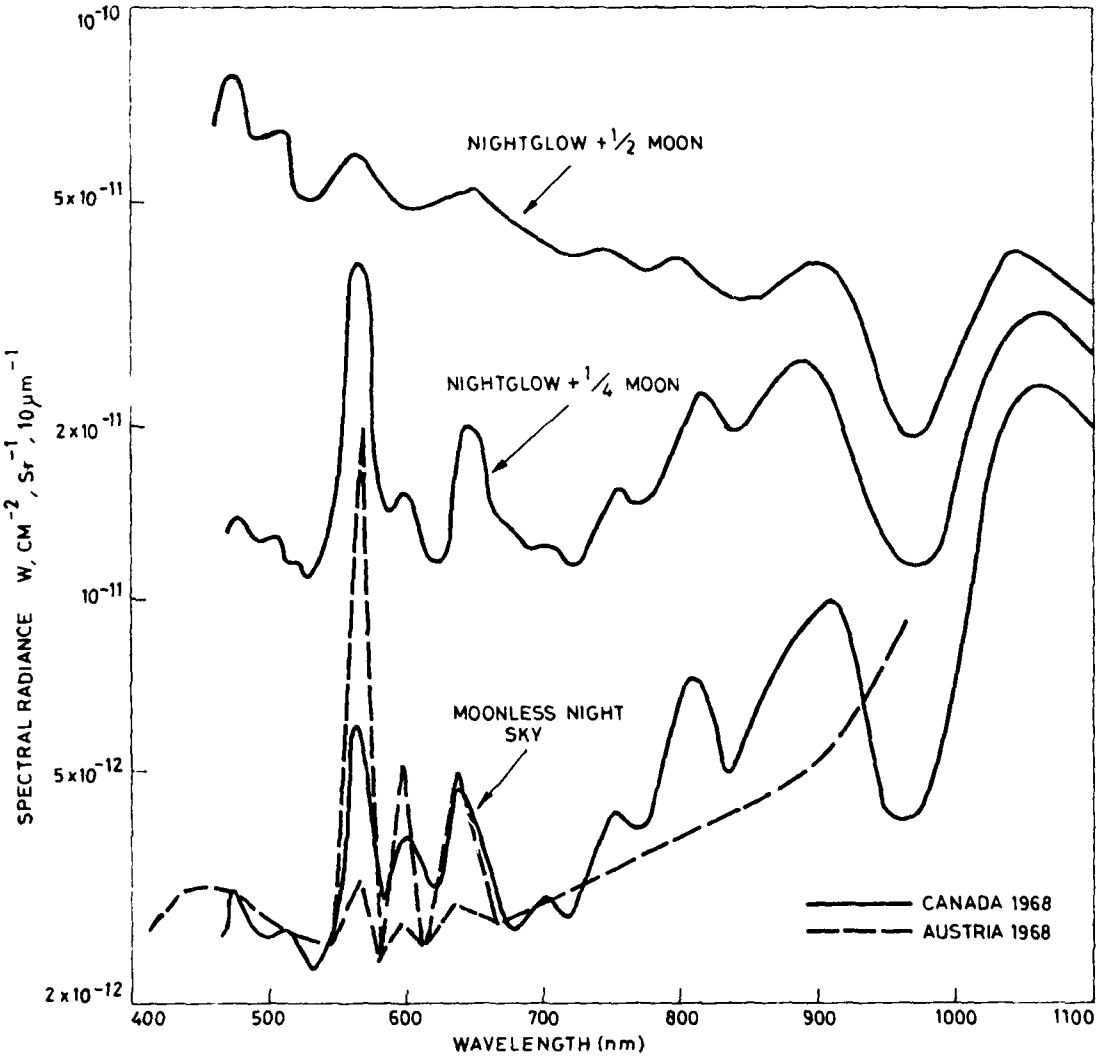

Figure 1. Measured night sky spectra

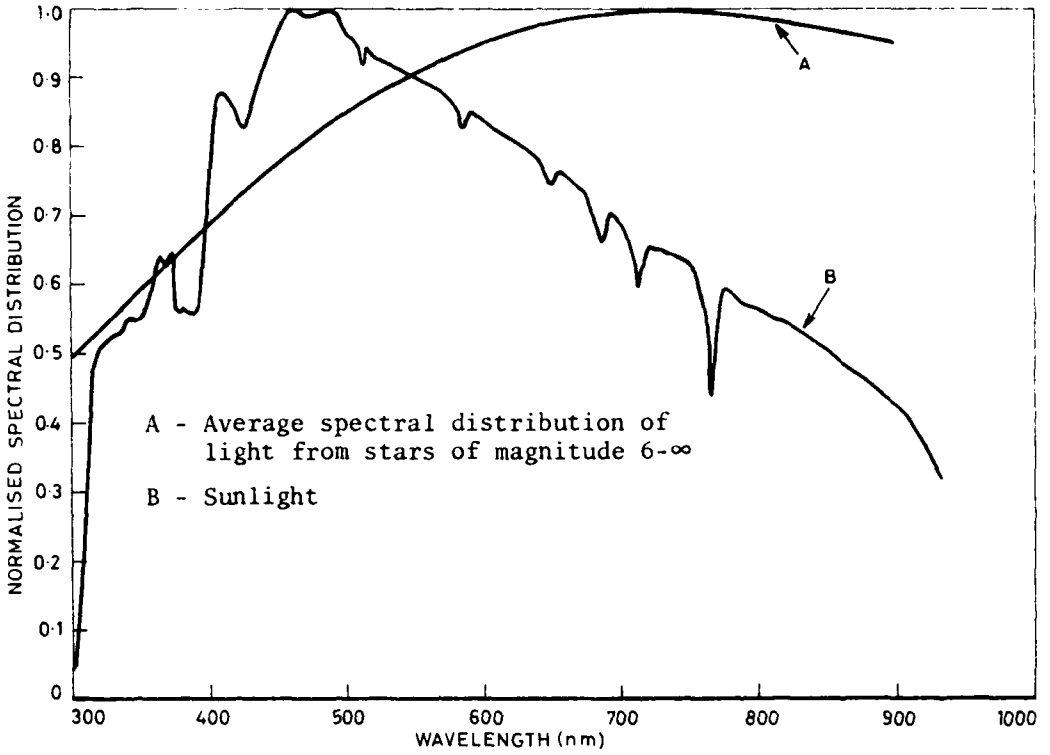

Figure 2. Spectral distribution of sunlight and weak starlight

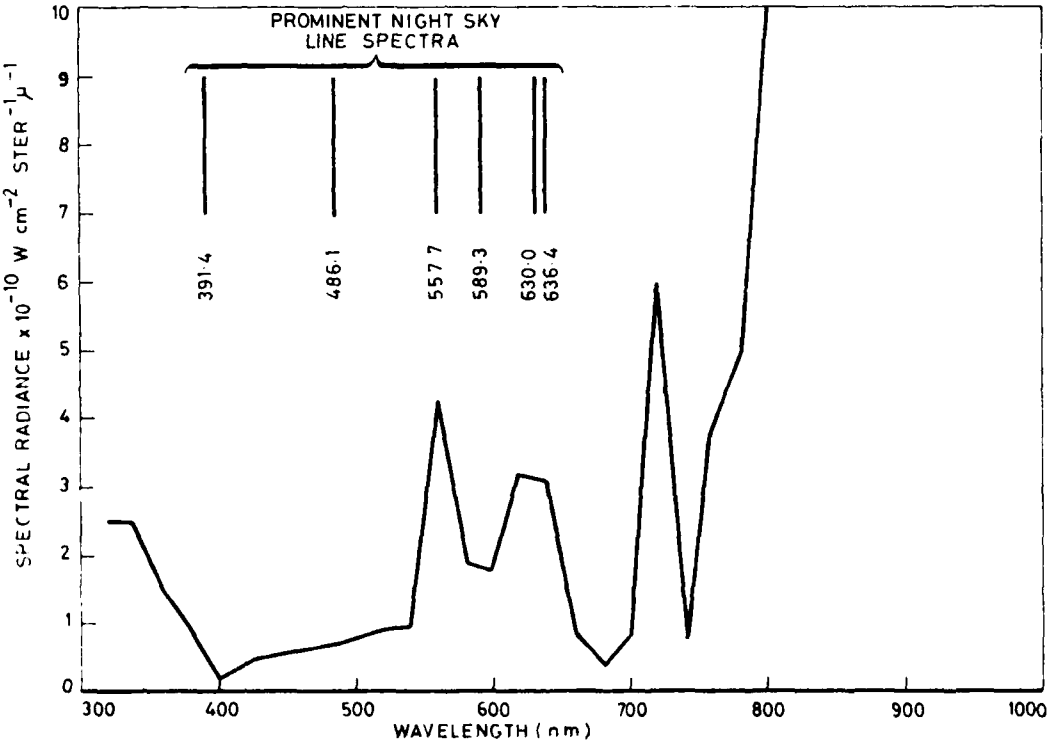

Figure 3. The night sky spectral radiance due to airglow

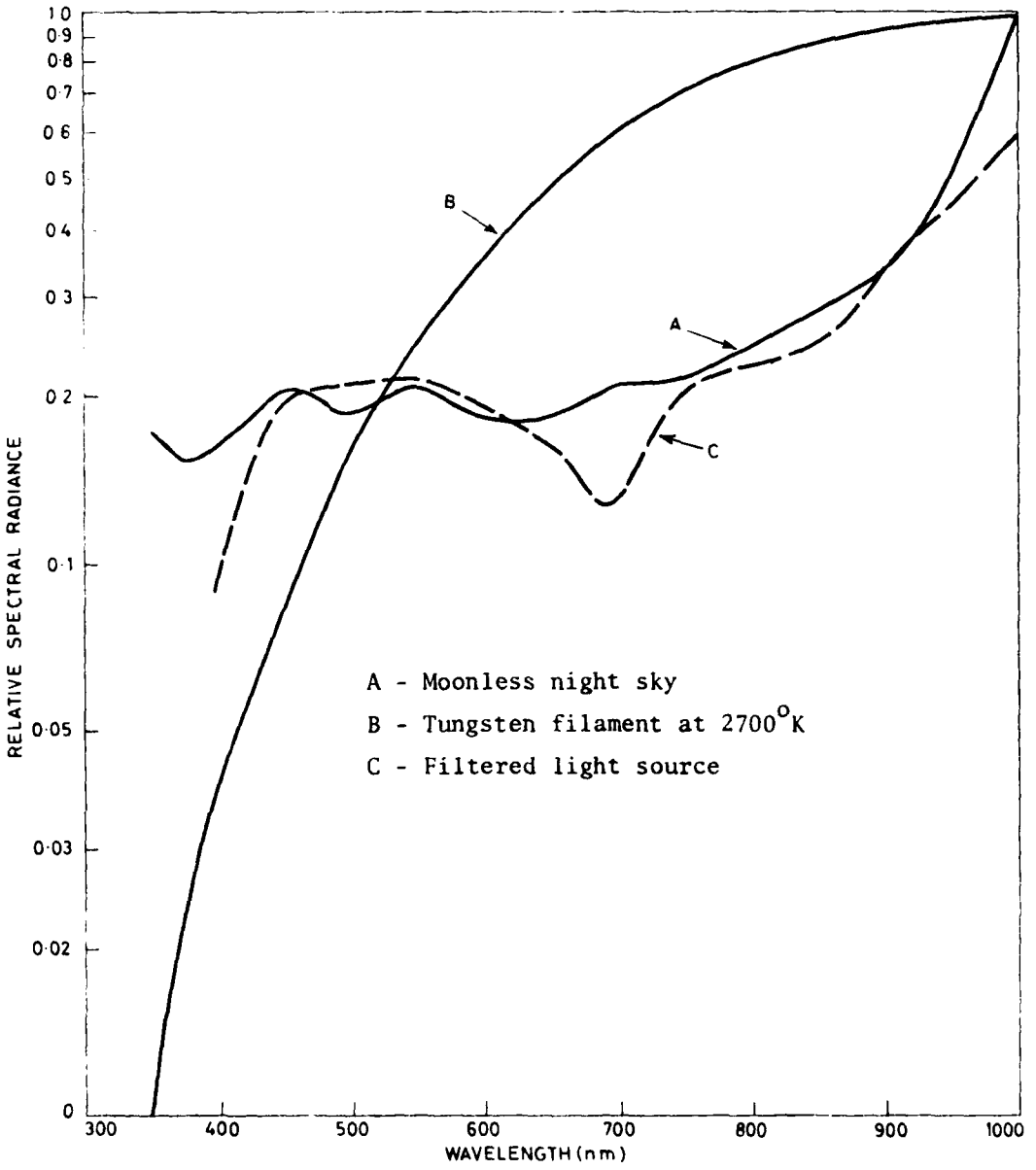

Figure 4. Relative spectral radiance of night sky and tungsten filament

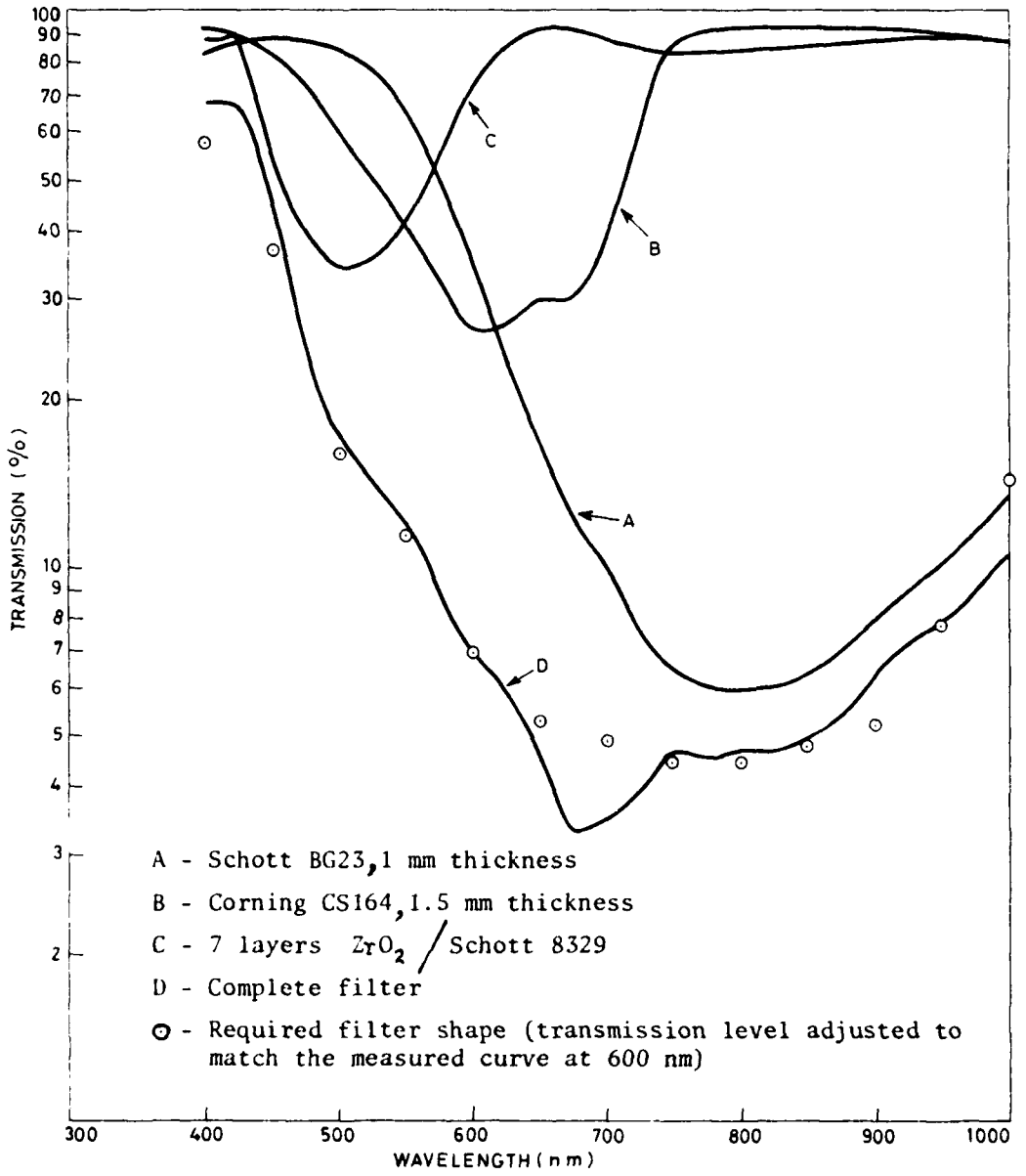

Figure 5. Spectral transmission of filter and components

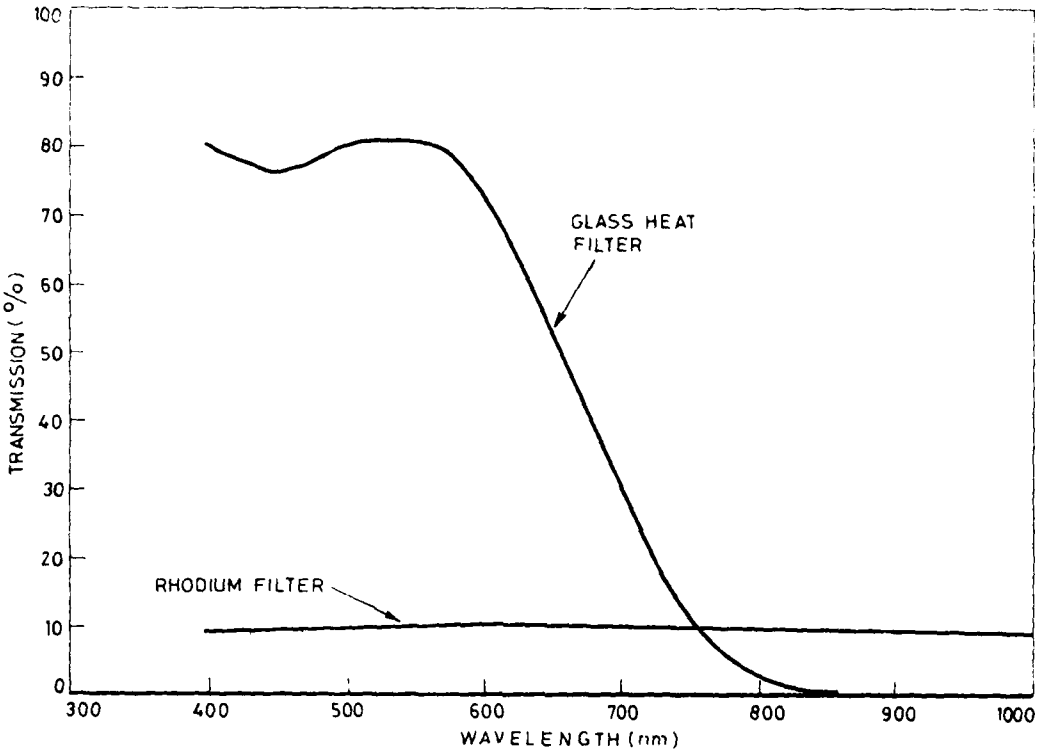

Figure 6. Spectral transmission of heat filters

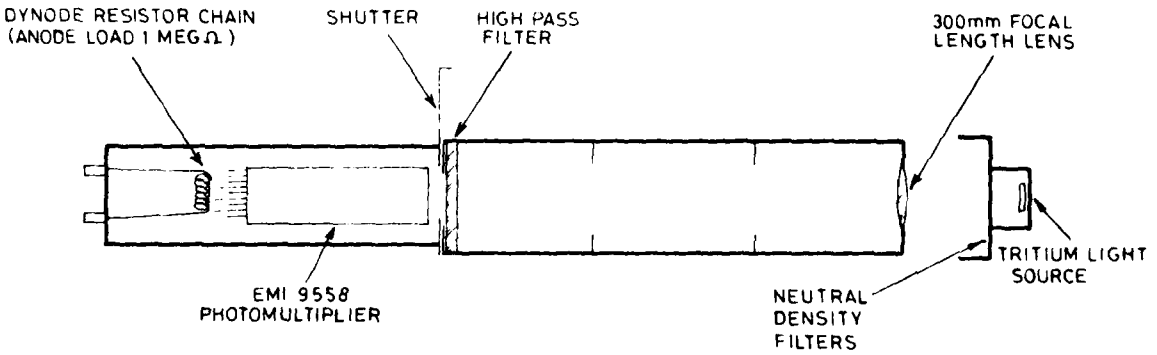

Figure 7. Schematic diagram of night sky radiometer

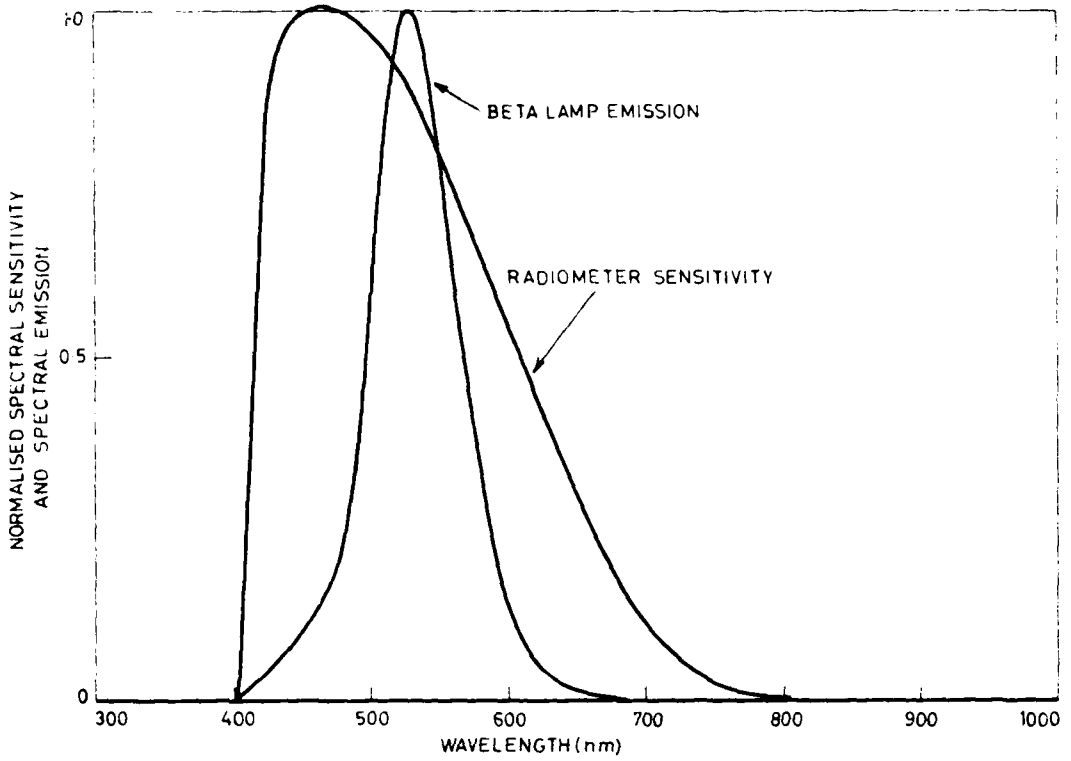

Figure 8. Radiometer spectral sensitivity and Beta lamp spectral emission

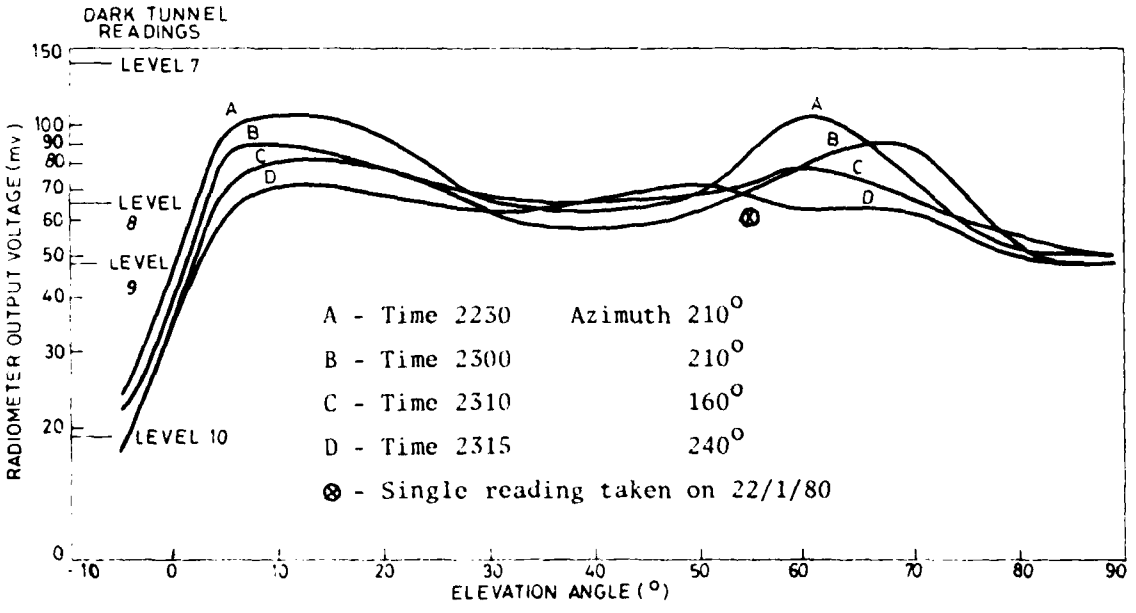

Figure 9. Night sky measurements at Waitpinga beach

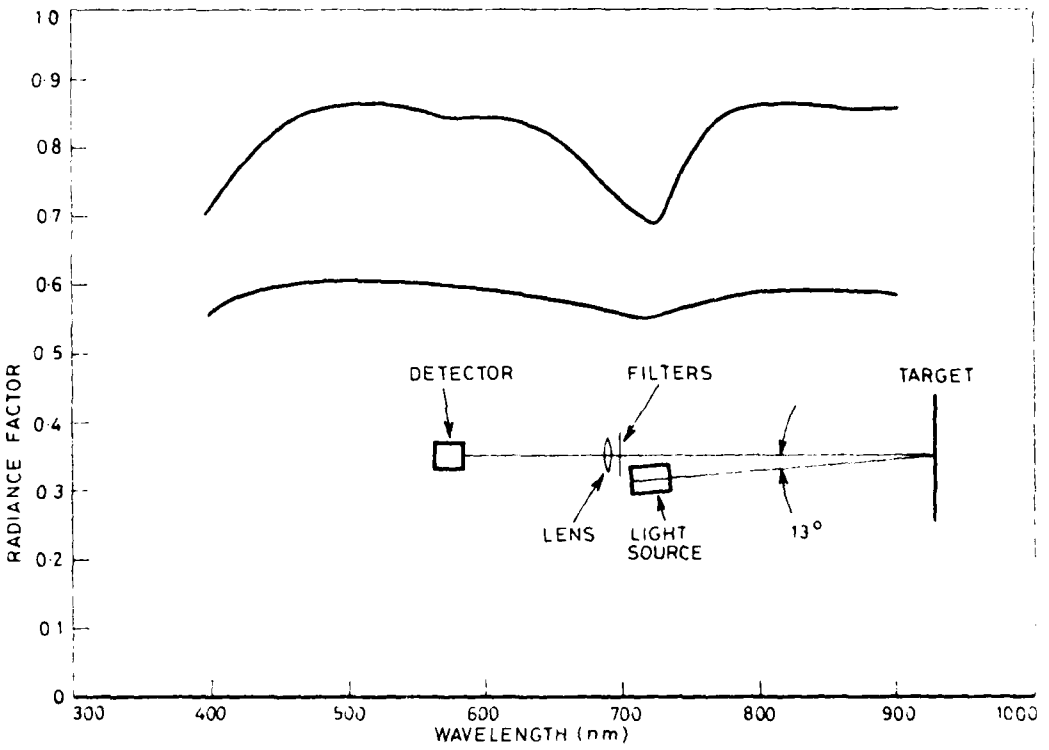

Figure 10. Radiance factor of dark tunnel end wall

DISTRIBUTION

	Copy No.
EXTERNAL	
In United Kingdom	
Defence Scientific and Technical Representative, London	No copy
British Library Lending Division	1
In United States of America	
Counsellor, Defence Science, Washington	No copy
National Technical Information Service	2
NASA Scientific and Technical Information Office	3
Engineering Societies Library	4
In Australia	
Chief Defence Scientist	5
Deputy Chief Defence Scientist	6
Director, Joint Intelligence Organisation (DDSTI)	7
Controller, Projects and Analytical Studies	8
Superintendent, Science and Technology Programmes	9
Defence Information Services Branch (for microfilming)	10
Defence Information Services Branch for:	
United Kingdom, Ministry of Defence, Defence Research Information Centre (DRIC)	11
United States, Defense Technical Information Center	12 - 23
Canada, Department of National Defence, Defence Science Information Service	24
New Zealand, Ministry of Defence	25
Australian National Library	26
Director General, Army Development (NCO) for:	
UK ABCA representative, Canberra	27
Canada ABCA representative, Canberra	28
US ABCA representative, Canberra	29
Director, Industry Development Regional Office, Adelaide	30

Navy Scientific Adviser	31
Director of Submarine Policy	32
Director of Submarine Maintenance and Repair	33
The Commander First Australian Submarine Squadron	34
Superintendent, RAN Research Laboratory	35
Defence Library, Campbell Park	36
Library, Aeronautical Research Laboratories	37
Library, Materials Research Laboratories	38
WITHIN DRCS	
Chief Superintendent, Electronics Research Laboratory	39
Superintendent, Navigation and Surveillance Division	40
Senior Principal Research Scientist, Surveillance	41
Principal Officer, Optical Techniques Group	42
Principal Officer, Night Vision Group	43
Mr N.S. Bromilow, Optical Techniques Group	44
Mr H.H. Brophy, Optical Techniques Group	45
Mr M.S. Brown, Optical Techniques Group	46 - 50
Mr M.W. Rossiter, Optical Techniques Group	51
Mr J.R. Venning, Optical Techniques Group	52
Mr E.D. Anderson, Optical Techniques Group	53
Mr M.R. Meharry, Night Vision Group	54
DRCS Library	55 - 56
Spares	57 - 61

The official documents produced by the Laboratories of the Defence Research Centre Salisbury are issued in one of five categories: Reports, Technical Reports, Technical Memoranda, Manuals and Specifications. The purpose of the latter two categories is self-evident, with the other three categories being used for the following purposes:

Reports	:	documents prepared for managerial purposes.
Technical *Reports*	:	records of scientific and technical work of a permanent value intended for other scientists and technologists working in the field.
Technical Memoranda	:	intended primarily for disseminating information within the DSTO. They are usually tentative in nature and reflect the personal views of the author.